Available online at www.sciencedirect.com
ScienceDirect
Journal of Sound and Vibration 324 (2009) 773–797
JOURNAL OF SOUND AND VIBRATION
www.elsevier.com/locate/jsvi

Effect of rotation and imperfection on reflection and transmission of plane waves in anisotropic generalized thermoelastic media

Rajneesh Kumar[a,*], Manjeet Singh[b]

[a]Department of Mathematics, Kurukshetra University, Kurukshetra-136 119, Haryana, India
[b]Department of Mathematics, S.U.S. Govt. College, Matak Majri, Indri, Karnal, Haryana, India

Received 28 April 2007; received in revised form 7 October 2008; accepted 22 February 2009
Handling Editor: L.G. Tham
Available online 8 April 2009

Abstract

The present investigation is concerned with the propagation of plane waves at an imperfectly bonded interface of two orthotropic generalized thermoelastic rotating half-spaces with different elastic and thermal properties. The thermoelastic theory with one relaxation time developed by Lord and Shulman [A generalized dynamical theory of thermoelasticity, *J. Mech. Phys. Solids* 15 (1967) 299–309] is used to study the problem. The reflection and transmission coefficients of Quasi Longitudinal (QL-) wave, Quasi Thermal (T-mode) wave and Quasi Transverse (QT-) wave have been derived. The effect of rotation has been studied on the velocities of different waves. Some special cases of boundaries i.e. normal stiffness, transverse stiffness, thermal contact conductance, slip boundary and welded contact boundary have been deduced from an imperfect one. Impact of different boundaries has been studied graphically. It is observed that thermal properties, rotation and imperfect boundary have significant effect on the propagation of waves.

1. Introduction

Debonding and imperfect contact however are known to exist in composites, be in the domain of electrical, thermal conduction or elasticity. For example, even grain boundaries in polycrystalline materials are not perfect because of misfit of the atomic structures of two neighboring grains. In this case dislocation may form on the interface and the atomic structure becomes different than in the bulk medium. This interface imperfection may be felt only at very high frequencies. Another example of formation of a thin interface layer occurs when two solids are bonded together either by a thin layer of another materials, for example, glue or by some metallurgical process.

The popular model, which was adopted in the present study, is the linear spring like model, in which a thin layer of interphase material is introduced near the interface. In the limit of vanishing layer thickness, the

*Corresponding author.
E-mail addresses: rajneesh_kuk@rediffmail.com (R. Kumar), manjeet_kuk@indiatimes.com (M. Singh).

0022-460X/$ - see front matter © 2009 Elsevier Ltd. All rights reserved.
doi:10.1016/j.jsv.2009.02.024

Nomenclature

c_{ij}	isothermal elastic parameters	α_i	coefficients of linear thermal expansion
ρ	density	t_0	relaxation time
C^*	specific heat at constant strain	k	wave number
T_0	the initial uniform temperature	c	phase velocity
σ_{ij}	components of stress tensor	ω	circular frequency
e_{ij}	components of strain tensor	t	time
		T	absolute temperature

interfacial tractions become continuous, but the displacement at either side of the interface layer become discontinuous, the jump in displacement being linearly proportional to the interfacial tractions and in the field of thermal conduction, the finite difference in temperature between two dissimilar materials is proportional to the heat flux at the interface. The boundary between the solids may behave as slip, perfect or neither, depending on the properties of this layer, as has been demonstrated by Rokhlin and Marom [11], and its state significantly affects thermoelastic wave reflection and interface mechanical behavior.

Significant work has been done to describe the physical conditions on the interface by different mechanical boundary conditions by different investigators. Notable among them are Jones and Whittier [2], Nayfeh and Nassar [4], Rokhlin et al. [5], Rokhlin [8], Baik and Thomson [9], Angel and Achenbach [10], Pilarski and Rose [12], Lovrentyev and Rokhlin [17], Laungvichcharoen et al. [22], Wang et al. [24], Ueda et al. [28].

The heat equation for both coupled and uncoupled theories is of the diffusion type, predicting infinite speeds of propagation for thermal waves, contrary to physical observations. Lord and Shulman [1] introduced the theory of generalized thermoelasticity with one relaxation time by postulating a new law of heat conduction to replace the classical Fourier's law. This law contains the heat flux vector as well as its time derivative. In addition it contains a new constant that acts as relaxation time. The heat equation of this theory is of wave type, ensuring finite speeds of propagation for thermal and elastic waves. The remaining governing equations for this theory, namely the equation of motion and the constitutive relation, remain the same as those for the coupled and uncoupled theories. Dhaliwal and Sherief [7] extended this theory to an anisotropic media. The second generalization was developed by Green and Lindsay [3] and is known as G–L theory. This theory contains two constants that act as relaxation times and modifies all the equations of coupled theory not the heat conduction equation only. The two theories both ensure finite speeds of propagation for thermal wave.

Many authors contribute their efforts in studying the wave propagation in different types of medium, few among them are Sharma [13], Sharma and Singh [14], Sinha and Elsibai [15,16], Abd-Alla and Al-Dawy [18], Verma [19], Singh [20], Othman [21], Kumar and Sharma [23], Othman [25], Baksi and Bera [26], Sharma and Thakur [27], Sharma and Othman [29].

This spring like model has been adopted in the present work between two generalized thermoelastic solids as has been represented by the boundary conditions in the text. K_n, K_t, K_c used in the boundary conditions are spring constant type material parameters. $K_n \to \infty$, $K_t \to \infty$, $K_c \to \infty$ implies the continuity of displacement components and temperature distribution and therefore the two solids are perfectly bonded together or to say that the two solids are in welded contact (WC). At the other extreme $K_n \to 0$, $K_t \to 0$, $K_c \to 0$ implies that the two solids are completely unbonded and $x_3 = 0$ is a free surface. So any finite positive value of these so-called interface parameters defines an imperfect interface.

This study is motivated by the need for a better understanding of the role of interfaces on the propagation of thermoelastic plane waves and how rotation plays its role when studied with imperfection. Therefore different boundaries has been developed and impact of different boundaries on the reflection and refraction of thermoelastic plane waves in orthotropic generalized thermoelastic rotating medium with one relaxation time has been studied.

2. Basic equations

Consider a homogeneous orthotropic thermoelastic medium with one relaxation time. It has two plane of symmetry and its elastic properties are defined by nine elastic moduli. The generalized Hooke's law can be expressed in the form

$$\sigma_{11} = c_{11}e_{11} + c_{12}e_{22} + c_{13}e_{33} - \beta_1 T, \tag{1}$$

$$\sigma_{22} = c_{12}e_{11} + c_{22}e_{22} + c_{23}e_{33} - \beta_2 T, \tag{2}$$

$$\sigma_{33} = c_{13}e_{11} + c_{23}e_{22} + c_{33}e_{33} - \beta_3 T, \tag{3}$$

$$\sigma_{23} = 2c_{44}e_{23}, \tag{4}$$

$$\sigma_{13} = 2c_{55}e_{13}, \tag{5}$$

$$\sigma_{12} = 2c_{66}e_{12}, \tag{6}$$

where σ_{ij} is the stress tensor and e_{ij} the strain tensor. Further

$$2e_{ij} = \frac{\partial u_i}{\partial x_j} + \frac{\partial u_j}{\partial x_i} \quad (i,j = 1,2,3), \tag{7}$$

u_i being the displacement vector.

The equations of motion and heat conduction equation in an orthotropic non-rotating thermoelastic medium with one relaxation time without body forces and heat sources are

$$\frac{\partial}{\partial x_j}\sigma_{ij} = \rho \frac{\partial^2 u_i}{\partial t^2} \quad (i,j = 1,2,3), \tag{8}$$

$$K_1 \frac{\partial^2 T}{\partial x_1^2} + K_2 \frac{\partial^2 T}{\partial x_2^2} + K_3 \frac{\partial^2 T}{\partial x_3^2} - T_0 \left(\frac{\partial}{\partial t} + t_0 \frac{\partial^2}{\partial t^2}\right)\left(\beta_1 \frac{\partial u_1}{\partial x_1} + \beta_2 \frac{\partial u_2}{\partial x_2} + \beta_3 \frac{\partial u_3}{\partial x_3}\right) = \rho C^* \left(\frac{\partial T}{\partial t} + t_0 \frac{\partial^2 T}{\partial t^2}\right), \tag{9}$$

where

$$\beta_1 = c_{11}\alpha_1 + c_{12}\alpha_2 + c_{13}\alpha_3, \quad \beta_2 = c_{12}\alpha_1 + c_{22}\alpha_2 + c_{23}\alpha_3, \quad \beta_3 = c_{13}\alpha_1 + c_{23}\alpha_2 + c_{33}\alpha_3.$$

3. Formulation of the problem

We consider two homogeneous orthotropic generalized thermoelastic solid half-spaces being in contact with each other at a plane surface, which we designate as the plane $x_3 = 0$ of a rectangular cartesian co-ordinate system $OX_1X_2X_3$. The medium is rotating with an angular velocity $\vec{\Omega} = \Omega\hat{n}$, where $\hat{n}$ is the unit vector representing the direction of rotation. In the present problem, $\vec{\Omega} = (\Omega, 0, 0)$.

The equation of motion in rotating frame of reference has two additional terms (i) centripetal acceleration $\vec{\Omega} \times (\vec{\Omega} \times \vec{u})$ due to time varying motion only (ii) the Coriolis acceleration $2\vec{\Omega} \times \dot{\vec{u}}$. So Eq. (8) can be modified in rotating medium as

$$\frac{\partial}{\partial x_j}\sigma_{ij} = \rho\left[\frac{\partial^2 u_i}{\partial t^2} + \{\vec{\Omega} \times (\vec{\Omega} \times \vec{u})\}_i + (2\vec{\Omega} \times \dot{\vec{u}})_i\right] \quad (i,j = 1,2,3). \tag{10}$$

We consider thermoelastic plane waves in x_2x_3-plane with wave front parallel to x_1 axis and all the field variables depend on x_2, x_3 and t.

For the plane wave propagating in the x_2x_3-plane

$$u_i = u_i(x_2, x_3, t), \quad \frac{\partial}{\partial x_1} \equiv 0, \quad T = T(x_2, x_3, t). \tag{11}$$

From Eqs. (1)–(7) and (9)–(11), we obtain the equations of motion and heat conduction equation in a rotating medium without body forces and heat sources in terms of the displacements in the form

$$c_{66}\frac{\partial^2 u_1}{\partial x_2^2}+c_{55}\frac{\partial^2 u_1}{\partial x_3^2}=\rho\frac{\partial^2 u_1}{\partial t^2}, \tag{12}$$

$$c_{22}\frac{\partial^2 u_2}{\partial x_2^2}+c_{44}\frac{\partial^2 u_2}{\partial x_3^2}+(c_{23}+c_{44})\frac{\partial^2 u_3}{\partial x_2\partial x_3}=\rho\left[\frac{\partial^2 u_2}{\partial t^2}-\Omega^2 u_2-2\Omega\dot{u}_3\right]+\beta_2 T_{,2}, \tag{13}$$

$$c_{44}\frac{\partial^2 u_3}{\partial x_2^2}+c_{33}\frac{\partial^2 u_3}{\partial x_3^2}+(c_{23}+c_{44})\frac{\partial^2 u_2}{\partial x_2\partial x_3}=\rho\left[\frac{\partial^2 u_3}{\partial t^2}-\Omega^2 u_3-2\Omega\dot{u}_2\right]+\beta_3 T_{,3}, \tag{14}$$

$$K_2\frac{\partial^2 T}{\partial x_2^2}+K_3\frac{\partial^2 T}{\partial x_3^2}-T_0\left(\frac{\partial}{\partial t}+t_0\frac{\partial^2}{\partial t^2}\right)\left(\beta_2\frac{\partial u_2}{\partial x_2}+\beta_3\frac{\partial u_3}{\partial x_3}\right)=\rho C^*\left(\frac{\partial}{\partial t}+t_0\frac{\partial^2}{\partial t^2}\right)T, \tag{15}$$

From Eqs. (12)–(14), it is obvious that the u_1 motion representing SH waves is decoupled from the (u_2,u_3) motion.

Let $\vec{p}(0,p_2,p_3)$ denote the unit propagation vector, c the phase velocity and k the wave number of the plane waves propagating in x_2x_3-plane.

The plane wave solutions of Eqs. (13)–(15) are of the form

$$\begin{pmatrix}u_2\\u_3\\T\end{pmatrix}=\begin{pmatrix}A\\B\\C\end{pmatrix}\exp[\mathrm{i}k(ct-x_2p_2-x_3p_3)]. \tag{16}$$

Using Eq. (16) in Eqs. (13)–(15), we have

$$[\overline{U}-c^2(1+\Omega_1^2)]A+[\overline{V}-2\mathrm{i}\Omega_1c^2]B-\left(\frac{i}{k}\right)\overline{\beta}_2p_2C=0, \tag{17}$$

$$[\overline{V}+2\mathrm{i}\Omega_1c^2]A+[\overline{Z}-c^2(1+\Omega_1^2)]B-\left(\frac{i}{k}\right)\overline{\beta}_3p_3C=0, \tag{18}$$

$$\tau^*T_0c^2\overline{\beta}_2p_2A+\tau^*T_0c^2\overline{\beta}_3p_3B-\left(\frac{i}{k}\right)(\overline{W}-c^2C^*\tau^*)C=0, \tag{19}$$

where

$$\overline{U}(p_2,p_3)=\frac{c_{22}}{\rho}p_2^2+\frac{c_{44}}{\rho}p_3^2,\quad \overline{Z}(p_2,p_3)=\frac{c_{44}}{\rho}p_2^2+\frac{c_{33}}{\rho}p_3^2,$$

$$\overline{V}(p_2,p_3)=\left(\frac{c_{23}+c_{44}}{\rho}\right)p_2p_3,\quad \overline{W}(p_2,p_3)=\frac{K_2}{\rho}p_2^2+\frac{K_3}{\rho}p_3^2,$$

$$\overline{\beta}_2=\frac{\beta_2}{\rho},\quad \overline{\beta}_3=\frac{\beta_3}{\rho},$$

$$\tau^*=\frac{1}{\omega}(\tau_0-i),\quad \tau_0=t_0\omega,\quad \Omega_1=\frac{\Omega}{\omega}. \tag{20}$$

Eqs. (17)–(19) in A, B, C can have a nontrivial solution only if the determinant of their coefficients vanishes, i.e.

$$A_0\zeta^3+A_1\zeta^2+A_2\zeta+A_3=0, \tag{21}$$

where

$$A_0=\tau^*,$$

$$A_1 = \frac{-[(\overline{Z}+\overline{U})(1+\Omega_1^2)\tau^* + \overline{W}^*(1+\Omega_1^4-2\Omega_1^2) + \varepsilon\eta(1+\Omega_1^2)(p_2^2+\overline{\beta}^2 p_3^2)]}{(1+\Omega_1^4-2\Omega_1^2)},$$

$$A_2 = -\frac{[(-\overline{Z}\overline{U}+\overline{V}^2)\tau^* - \overline{W}^*(\overline{Z}+\overline{U})(1+\Omega_1^2) + 2\varepsilon\eta\overline{V}\,\overline{\beta}p_2p_3 - \varepsilon\eta(\overline{\beta}^2 p_3^2\overline{U}+\overline{Z}p_2^2)]}{(1+\Omega_1^4-2\Omega_1^2)},$$

$$A_3 = \frac{-\overline{W}^*(\overline{Z}\overline{U}-\overline{V}^2)}{(1+\Omega_1^4-2\Omega_1^2)},$$

with

$$\zeta = c^2, \quad \overline{W}^* = \frac{\overline{W}}{C^*}, \quad \varepsilon = \frac{\beta_2^2 T_0}{\rho C^* c_{22}}, \quad \eta = \frac{\tau c_{22}}{\rho}, \quad \overline{\beta} = \frac{\beta_3}{\beta_2}.$$

To solve Eq. (21) we assume $\xi = \tau^*\zeta + (A_1/3)$, yielding

$$\xi^3 + 3H\xi + G = 0, \tag{22}$$

where

$$H = \frac{(3\tau^* A_2 - A_1^2)}{9}, \quad G = \frac{(27\tau^{*2}A_3 - 9\tau^* A_1 A_2 + 2A_1^3)}{27}$$

Roots of Eq. (22) are given by

$$\xi_1 = h_1 + h_2, \quad \xi_2 = h_1 g + h_2 g^2, \quad \xi_3 = h_1 g^2 + h_2 g,$$

with

$$h_1^3 = \frac{[-G + (G^2+4H^3)^{1/2}]}{2}, \quad h_2^3 = \frac{[-G - (G^2+4H^3)^{1/2}]}{2}, \quad g = \frac{(-1 \pm \mathrm{i}\sqrt{3})}{2}.$$

So, three roots of Eq. (21) are given by

$$\zeta_1 = \frac{[\xi_1 - (A_1/3)]}{\tau^*}, \quad \zeta_2 = \frac{[\xi_2 - (A_1/3)]}{\tau^*}, \quad \zeta_3 = \frac{[\xi_3 - (A_1/3)]}{\tau^*}.$$

The velocities of three waves (QL-wave, T-mode wave, QT-wave) are given by $(\zeta_1)^{1/2}, (\zeta_2)^{1/2}, (\zeta_3)^{1/2}$ and named as c_1, c_2, c_3, respectively.

4. Reflection and transmission

Consider a homogeneous, orthotropic rotating generalized thermoelastic half-space occupying the region $x_3 > 0$ in imperfect bonded contact with another homogeneous orthotropic rotating generalized thermoelastic half-space occupying the region $x_3 < 0$. Incident QL- or QT- or T-mode wave at the interface will generate reflected QL-, QT-, T-mode waves in the half-space $x_3 > 0$ and transmitted QL-, QT-, T-mode waves in the half-space $x_3 < 0$ as shown in Fig. 1.

$$u_2 = \sum_{j=1}^{6} A_j \mathrm{e}^{\mathrm{i}P_j}, \quad u_3 = \sum_{j=1}^{6} B_j \mathrm{e}^{\mathrm{i}P_j} \quad \text{for } x_3 > 0,$$

$$u_2' = \sum_{j=7}^{9} A_j \mathrm{e}^{\mathrm{i}P_j}, \quad u_3' = \sum_{j=7}^{9} B_j \mathrm{e}^{\mathrm{i}P_j} \quad \text{for } x_3 < 0,$$

$$T = \sum_{j=1}^{6} C_j \mathrm{e}^{\mathrm{i}P_j}, \quad T' = \sum_{j=7}^{9} C_j \mathrm{e}^{\mathrm{i}P_j}. \tag{23}$$

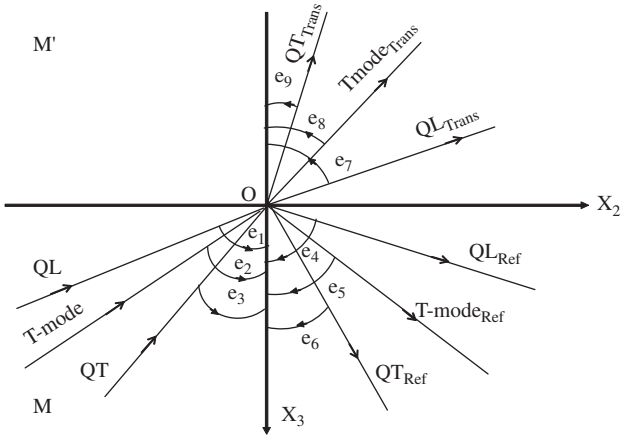

Fig. 1. Geometry of the problem.

where

$$P_j = \omega[t - (x_2 \sin e_j - x_3 \cos e_j)/c_j], \quad \text{for } j = 1,2,3,7,8,9,$$

$$P_j = \omega[t - (x_2 \sin e_j + x_3 \cos e_j)/c_j], \quad \text{for } j = 4,5,6, \tag{24}$$

ω being the angular frequency. We distinguish quantities corresponding to various waves by using the subscript 1 for incident QL-waves, 2 for incident T-mode waves, 3 for incident QT-waves, 4 for reflected QL-waves, 5 for reflected T-mode waves, 6 for reflected QT-waves, 7 for transmitted QL-waves, 8 for transmitted T-mode waves and 9 for transmitted QT-waves. Thus, for example, for the incident QL-waves, c_1 denotes the phase velocity, e_1 the angle of incidence, P_1 (x_2, x_3, t), the phase factor, A_1 the amplitude of the u_2 component of the displacement and B_1 that of the u_3 component of the displacement. We attach a prime to denote the variables in the half-space $x_3 < 0$, i.e. the displacement components are denoted by u_2' and u_3'.

Since each of the incident QL-, incident T-mode, Incident QT-, reflected QL-, reflected T-mode, reflected QT-, transmitted QL-, transmitted T-mode and transmitted QT-waves must satisfy the equations of motion and heat conduction equation, we have from Eqs. (17) and (18):

$$A_j = F_j B_j, \quad C_j = F_j^* B_j \quad (j = 1, \ldots, 9)$$

$$F_j = \frac{[\overline{Z}_j - c_j^2(1+\Omega_1^2)]\beta_2 p_2 - (\overline{V}_j - 2i\Omega_1 c_j^2)\beta_3 p_3}{[\overline{U}_j - c_j^2(1+\Omega_1^2)]\beta_3 p_3 - (\overline{V}_j + 2i\Omega_1 c_j^2)\beta_2 p_2},$$

$$F_j^* = \frac{[\overline{Z}_j - c_j^2(1+\Omega_1^2)][\overline{U}_j - c_j^2(1+\Omega_1^2)] - \left(V_j^2 + 4\Omega_1^2 c_j^4\right)}{\frac{i}{k}[\{\overline{U}_j - c_j^2(1+\Omega_1^2)\}\overline{\beta}_3 p_3 - (\overline{V}_j + 2i\Omega_1 c_j^2)\overline{\beta}_2 p_2]}, \tag{25}$$

The expressions for $\overline{U}_j, \overline{V}_j, \overline{Z}_j$ are obtained from the expressions for $\overline{U}, \overline{V}, \overline{Z}$ given in Eq. (20) on substituting the values for (p_2,p_3). For incident QL-wave $p_2 = \sin e_1$, $p_3 = -\cos e_1$; for incident T-mode wave $p_2 = \sin e_2$, $p_3 = -\cos e_2$; for incident QT-wave $p_2 = \sin e_3$, $p_3 = -\cos e_3$; for reflected QL-wave $p_2 = \sin e_4$, $p_3 = \cos e_4$; for reflected T-mode wave $p_2 = \sin e_5$, $p_3 = \cos e_5$; for reflected QT-wave $p_2 = \sin e_6$, $p_3 = \cos e_6$; for transmitted QL-wave $p_2 = \sin e_7$, $p_3 = -\cos e_7$; for transmitted T-mode wave $p_2 = \sin e_8$, $p_3 = -\cos e_8$ and for transmitted QT-wave $p_2 = \sin e_9$, $p_3 = -\cos e_9$. We thus have

$$\overline{U}_1 = \frac{c_{22}}{\rho}\sin^2 e_1 + \frac{c_{44}}{\rho}\cos^2 e_1, \quad \overline{V}_1 = -\left(\frac{c_{23}+c_{44}}{\rho}\right)\sin e_1 \cos e_1, \quad \overline{Z}_1 = \frac{c_{44}}{\rho}\sin^2 e_1 + \frac{c_{33}}{\rho}\cos^2 e_1,$$

$$\overline{U}_4=\frac{c_{22}}{\rho}\sin^2 e_4+\frac{c_{44}}{\rho}\cos^2 e_4,\quad \overline{V}_4=\left(\frac{c_{23}+c_{44}}{\rho}\right)\sin e_4\cos e_4,\quad \overline{Z}_4=\frac{c_{44}}{\rho}\sin^2 e_4+\frac{c_{33}}{\rho}\cos^2 e_4,$$

$$\overline{U}_7=\frac{c'_{22}}{\rho'}\sin^2 e_7+\frac{c'_{44}}{\rho'}\cos^2 e_7,\quad \overline{V}_7=-\left(\frac{c'_{23}+c'_{44}}{\rho'}\right)\sin e_7\cos e_7,\quad \overline{Z}_7=\frac{c'_{44}}{\rho'}\sin^2 e_7+\frac{c'_{33}}{\rho'}\cos^2 e_7.$$

$(\overline{U}_2,\overline{V}_2,\overline{Z}_2)$ and $(\overline{U}_3,\overline{V}_3,\overline{Z}_3)$ are obtained from $(\overline{U}_1,\overline{V}_1,\overline{Z}_1)$ on replacing e_1 by e_2 and e_3, $(\overline{U}_5,\overline{V}_5,\overline{Z}_5)$ and $(\overline{U}_6,\overline{V}_6,\overline{Z}_6)$ are obtained from $(\overline{U}_4,\overline{V}_4,\overline{Z}_4)$ on replacing e_4 by e_5 and e_6, $(\overline{U}_8,\overline{V}_8,\overline{Z}_8)$ and $(\overline{U}_9,\overline{V}_9,\overline{Z}_9)$ are obtained from $(\overline{U}_7,\overline{V}_7,\overline{Z}_7)$ on replacing e_7 by e_8 and e_9.

5. Boundary conditions

We consider two bonded thermoelastic half-spaces as shown in Fig. 1. If the bonding is imperfect and the size and spacing between the imperfections is much smaller than the wavelength then at the interface, the total displacement field and temperature field given by Eq. (23) must satisfy the spring boundary conditions at $x_3=0$ [17]

$$\text{(i) } \sigma'_{33}=K_n[u_3-u'_3],\quad \text{(ii) } \sigma'_{23}=K_t[u_2-u'_2],$$

$$\text{(iii) } K'_3\frac{\partial T'}{\partial x_3}=K_c[T-T'],\quad \text{(iv) } \sigma'_{33}=\sigma_{33},$$

$$\text{(v) } \sigma'_{23}=\sigma_{23},\quad \text{(vi) } K'_3\frac{\partial T'}{\partial x_3}=K_3\frac{\partial T}{\partial x_3}. \tag{26}$$

where K_n, K_t are the normal and transverse stiffness coefficients of a unit thin layer thickness with dimension $\mathrm{N/m^3}$ and K_c is the thermal contact conductance (TCC) with dimension $\mathrm{W/m^2\,K}$.

The boundary conditions given by Eq. (26) must be satisfied for all values of x_2, so we have

$$\begin{aligned}P_1(x_2,0,t)=P_2(x_2,0,t)=P_3(x_2,0,t)=P_4(x_2,0,t)=P_5(x_2,0,t)\\ =P_6(x_2,0,t)=P_7(x_2,0,t)=P_8(x_2,0,t)=P_9(x_2,0,t).\end{aligned} \tag{27}$$

Then from Eqs. (24) and (27), we have

$$\frac{\sin e_1}{c_1}=\frac{\sin e_2}{c_2}=\frac{\sin e_3}{c_3}=\frac{\sin e_4}{c_4}=\frac{\sin e_5}{c_5}=\frac{\sin e_6}{c_6}=\frac{\sin e_7}{c_7}=\frac{\sin e_8}{c_8}=\frac{\sin e_9}{c_9}=\frac{1}{c} \tag{28}$$

which corresponds to the Snell's law in the present case.

Here $e_1=e_4$, $e_2=e_5$ and $e_3=e_6$, i.e. the angle of incidence is equal to the angle of reflection in the orthotropic case, so the velocity of all reflected waves are equal to their corresponding incident wave, i.e. $c_1=c_4$, $c_2=c_5$ and $c_3=c_6$.

Making use of Eqs. (25), (27) and (28), the boundary conditions (26) yield

$$a_1B_1+a_2B_2+a_3B_3+a_4B_4+a_5B_5+a_6B_6+a_7B_7+a_8B_8+a_9B_9=0, \tag{29}$$

$$b_1B_1+b_2B_2+b_3B_3+b_4B_4+b_5B_5+b_6B_6+b_7B_7+b_8B_8+b_9B_9=0, \tag{30}$$

$$d_1B_1+d_2B_2+d_3B_3+d_4B_4+d_5B_5+d_6B_6+d_7B_7+d_8B_8+d_9B_9=0, \tag{31}$$

$$e_1B_1+e_2B_2+e_3B_3+e_4B_4+e_5B_5+e_6B_6+e_7B_7+e_8B_8+e_9B_9=0, \tag{32}$$

$$f_1B_1+f_2B_2+f_3B_3+f_4B_4+f_5B_5+f_6B_6+f_7B_7+f_8B_8+f_9B_9=0, \tag{33}$$

$$g_1B_1+g_2B_2+g_3B_3+g_4B_4+g_5B_5+g_6B_6+g_7B_7+g_8B_8+g_9B_9=0, \tag{34}$$

where

$$a_\ell=K_n\quad(\ell=1,\ldots,6),$$

$$a_\ell = -\left[K_n - c'_{23}\frac{\omega \sin e_\ell}{c_\ell}F_\ell + c'_{33}\frac{\omega \cos e_\ell}{c_\ell} - \beta'_3 F^*_\ell\right] \quad (\ell = 7,\ldots,9),$$

$$b_\ell = K_t F_\ell \quad (\ell = 1,\ldots,6),$$

$$b_\ell = -\left[K_t F_\ell + c'_{44}\left(\frac{\omega \cos e_\ell}{c_\ell}F_\ell - \frac{\omega \sin e_\ell}{c_\ell}\right)\right] \quad (\ell = 7,\ldots,9),$$

$$d_\ell = K_c F^*_\ell \quad (\ell = 1,\ldots,6),$$

$$d_\ell = -\left[K_c F^*_\ell + K'_3 F^*_\ell \frac{\omega \cos e_\ell}{c_\ell}\right] \quad (\ell = 7,\ldots,9),$$

$$e_\ell = -c_{23}\frac{\omega \sin e_\ell}{c_\ell}F_\ell + c_{33}\frac{\omega \cos e_\ell}{c_\ell} - \beta_3 F^*_\ell \quad (\ell = 1,\ldots,3),$$

$$e_\ell = -c_{23}\frac{\omega \sin e_\ell}{c_\ell}F_\ell - c_{33}\frac{\omega \cos e_\ell}{c_\ell} - \beta_3 F^*_\ell \quad (\ell = 4,\ldots,6),$$

$$e_\ell = c'_{23}\frac{\omega \sin e_\ell}{c_\ell}F_\ell - c'_{33}\frac{\omega \cos e_\ell}{c_\ell} + \beta'_3 F^*_\ell \quad (\ell = 7,\ldots,9),$$

$$f_\ell = c_{44}\left(\frac{\omega \cos e_\ell}{c_\ell}F_\ell - \frac{\omega \sin e_\ell}{c_\ell}\right) \quad (\ell = 1,\ldots,3),$$

$$f_\ell = -c_{44}\left(\frac{\omega \cos e_\ell}{c_\ell}F_\ell + \frac{\omega \sin e_\ell}{c_\ell}\right) \quad (\ell = 4,\ldots,6),$$

$$f_\ell = -c'_{44}\left(\frac{\omega \cos e_\ell}{c_\ell}F_\ell - \frac{\omega \sin e_\ell}{c_\ell}\right) \quad (\ell = 7,\ldots,9),$$

$$g_\ell = K_3 F^*_\ell \frac{\omega \cos e_\ell}{c_\ell} \quad (\ell = 1,\ldots,3), \quad g_\ell = -K_3 F^*_\ell \frac{\omega \cos e_\ell}{c_\ell} \quad (\ell = 4,\ldots,6),$$

$$g_\ell = -K'_3 F^*_\ell \frac{\omega \cos e_\ell}{c_\ell} \quad (\ell = 7,\ldots,9).$$

Incident QL-wave: In the case of Incident QL-wave, $A_2 = A_3 = B_2 = B_3 = C_2 = C_3 = 0$ and A_1, B_1, C_1 are supposed to be known. Eqs. (29)–(34) will constitute a set of six simultaneous equations in six unknowns, namely, $B_4, B_5, B_6, B_7, B_8, B_9$ and these can be solved by Cramer's rule and we have

$$\frac{B_\ell}{B_1} = \frac{\Delta^p_\ell}{\Delta} \quad (\ell = 4,5,6,7,8,9), \tag{35}$$

where Δ and Δ^p_ℓ are defined in Appendix A. From Eq. (25), we have

$$\frac{A_\ell}{A_1} = \frac{F_\ell}{F_1}\left(\frac{B_\ell}{B_1}\right) = \frac{F_\ell}{F_1}\left(\frac{\Delta^p_\ell}{\Delta}\right) \quad (\ell = 4,5,6,7,8,9), \tag{36}$$

$$\frac{C_\ell}{C_1} = \frac{F^*_\ell}{F^*_1}\left(\frac{B_\ell}{B_1}\right) = \frac{F^*_\ell}{F^*_1}\left(\frac{\Delta^p_\ell}{\Delta}\right) \quad (\ell = 4,5,6,7,8,9), \tag{37}$$

Incident T-mode wave: For Incident T-mode wave, $A_1 = A_3 = B_1 = B_3 = C_1 = C_3 = 0$ and A_2, B_2, C_2 are supposed to be known and Eqs. (29)–(34) will form a set of six simultaneous equations in six unknowns,

namely, $B_4, B_5, B_6, B_7, B_8, B_9$ and solving by Cramer's rule, we obtain

$$\frac{B_\ell}{B_2} = \frac{\Delta_\ell^T}{\Delta} \quad (\ell = 4,5,6,7,8,9), \tag{38}$$

where Δ and Δ_ℓ^T are defined in Appendix A. From Eq. (25), we have

$$\frac{A_\ell}{A_2} = \frac{F_\ell}{F_2}\left(\frac{B_\ell}{B_2}\right) = \frac{F_\ell}{F_2}\left(\frac{\Delta_\ell^T}{\Delta}\right) \quad (\ell = 4,5,6,7,8,9), \tag{39}$$

$$\frac{C_\ell}{C_2} = \frac{F_\ell^*}{F_2^*}\left(\frac{B_\ell}{B_2}\right) = \frac{F_\ell^*}{F_2^*}\left(\frac{\Delta_\ell^T}{\Delta}\right) \quad (\ell = 4,5,6,7,8,9). \tag{40}$$

Incident QT-wave: $A_1 = A_2 = B_1 = B_2 = C_1 = C_2 = 0$ and A_3, B_3, C_3 are supposed to be known in the case of Incident QT-wave. Solving Eqs. (28)–(33) by Cramer's rule, we will constitute a set of six simultaneous equations in six unknowns, i.e. $B_4, B_5, B_6, B_7, B_8, B_9$ obtaining amplitude ratios as

$$\frac{B_\ell}{B_3} = \frac{\Delta_\ell^S}{\Delta} \quad (\ell = 4,5,6,7,8,9), \tag{41}$$

where Δ and Δ_ℓ^S are defined in Appendix A. From Eq. (25), we have

$$\frac{A_\ell}{A_3} = \frac{F_\ell}{F_3}\left(\frac{B_\ell}{B_3}\right) = \frac{F_\ell}{F_3}\left(\frac{\Delta_\ell^S}{\Delta}\right) \quad (\ell = 4,5,6,7,8,9), \tag{42}$$

$$\frac{C_\ell}{C_3} = \frac{F_\ell^*}{F_3^*}\left(\frac{B_\ell}{B_3}\right) = \frac{F_\ell^*}{F_3^*}\left(\frac{\Delta_\ell^S}{\Delta}\right) \quad (\ell = 4,5,6,7,8,9). \tag{43}$$

In Eqs. (35)–(37), A_ℓ/A_1 are the amplitude ratios for the horizontal component of the displacement, B_ℓ/B_1 are the amplitude ratios for the normal component of the displacement and C_ℓ/C_1 are the amplitude ratios for the thermal parameter.

Similarly Eqs. (38)–(40) and (41)–(43) gives the amplitude ratios for incident T-mode and incident QT-waves, respectively.

The reflection coefficient for incident QL-wave can be expressed in the form

$$R_{PP} = \left(\frac{1+F_4^2+F_4^{*2}}{1+F_1^2+F_1^{*2}}\right)^{1/2}\frac{B_4}{B_1}, \quad R_{PT} = \left(\frac{1+F_5^2+F_5^{*2}}{1+F_1^2+F_1^{*2}}\right)^{1/2}\frac{B_5}{B_1}, \quad R_{PS} = \left(\frac{1+F_6^2+F_6^{*2}}{1+F_1^2+F_1^{*2}}\right)^{1/2}\frac{B_6}{B_1}, \tag{44}$$

The transmission coefficient for incident QL-wave can be expressed in the form

$$T_{PP} = \left(\frac{1+F_7^2+F_7^{*2}}{1+F_1^2+F_1^{*2}}\right)^{1/2}\frac{B_7}{B_1}, \quad T_{PT} = \left(\frac{1+F_8^2+F_8^{*2}}{1+F_1^2+F_1^{*2}}\right)^{1/2}\frac{B_8}{B_1}, \quad T_{PS} = \left(\frac{1+F_9^2+F_9^{*2}}{1+F_1^2+F_1^{*2}}\right)^{1/2}\frac{B_9}{B_1}. \tag{45}$$

Similar expressions can be written for the reflection and transmission coefficients for incident T-mode and incident QT-waves, by replacing the suffices 1 in the denominator by suffices 2 and 3, respectively. In the reflection and transmission coefficient subscript 1 represents the incident wave, subscript 2 represents the reflected and transmitted wave and in subscript P, T, S represent the QL-wave, T-mode wave, QT-wave, respectively.

6. Particular cases

Normal stiffness: This implies continuity of stress components, shear components of displacement and temperature distribution across the interface. If we put $K_n \neq 0$, $K_t \to \infty$, $K_c \to \infty$ in boundary conditions given by Eq. (26), then imperfect boundary correspond to the case of normal stiffness and the corresponding values of b_ℓ and d_ℓ as given by

$$b_\ell = F_\ell \ (\ell = 1,\ldots,6), \quad b_\ell = -F_\ell \ (\ell = 7,\ldots,9),$$

$$d_\ell = F_\ell^* \ (\ell = 1,\ldots,6), \quad d_\ell = -F_\ell^* \ (\ell = 7,\ldots,9).$$

Transverse stiffness: Applying $K_n \to \infty$, $K_t \neq 0$, $K_c \to \infty$ in boundary conditions given by Eq. (26), then we are left with transverse stiffness boundary, which implies continuity of stress components, normal components of displacement and temperature distribution across the interface. Corresponding modified values of a_ℓ and d_ℓ as given by

$$a_\ell = 1 \ (\ell = 1,\ldots,6), \quad a_\ell = -1 \ (\ell = 7,\ldots,9),$$

$$d_\ell = F_\ell^* \ (\ell = 1,\ldots,6), \quad d_\ell = -F_\ell^* \ (\ell = 7,\ldots,9).$$

Thermal contact conductance: This type of boundary is obtained if we put $K_n \to \infty$, $K_t \to \infty$, $K_c \neq 0$ in boundary conditions given by Eq. (26) and this implies continuity of stress components and components of

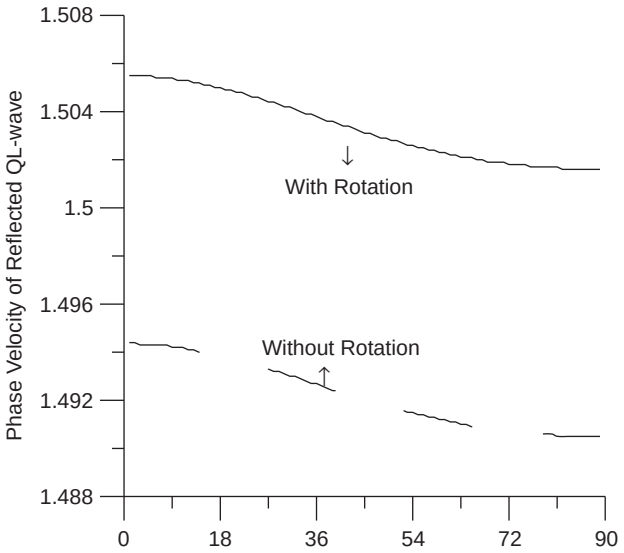

Fig. 2. Angle of incidence (in deg.)

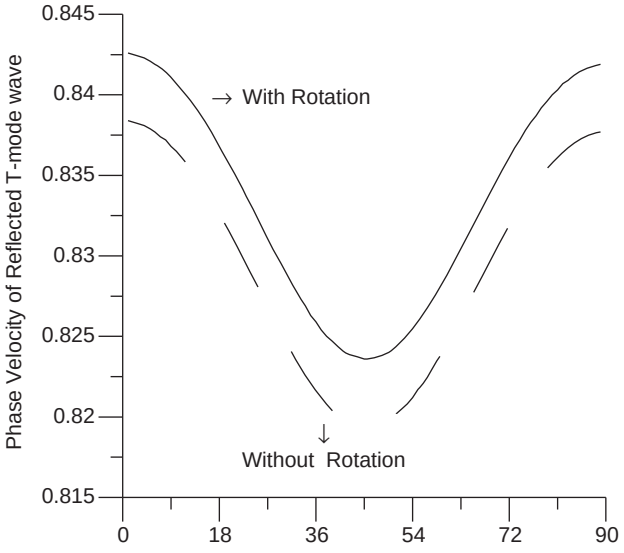

Fig. 3. Angle of incidence (in deg.)

displacement across the interface. Corresponding changed values of a_ℓ and b_ℓ as given by

$$a_\ell = 1 \ (\ell = 1, \ldots, 6), \quad a_\ell = -1 \ (\ell = 7, \ldots, 9),$$

$$b_\ell = F_\ell \ (\ell = 1, \ldots, 6), \quad b_\ell = -F_\ell \ (\ell = 7, \ldots, 9).$$

Slip boundary: In the boundary conditions given by Eq. (26), if we assume $K_n \to \infty$, $K_t = 0$, $K_c \to \infty$, then the imperfect boundary modifies to a slip one, which implies continuity of normal components of stress, normal components of displacement, temperature distribution and vanishing of transverse components of stresses. The changed values of a_ℓ, b_ℓ, d_ℓ and f_ℓ are

$$a_\ell = 1 \ (\ell = 1, \ldots, 6), \quad a_\ell = -1 \ (\ell = 7, \ldots, 9),$$

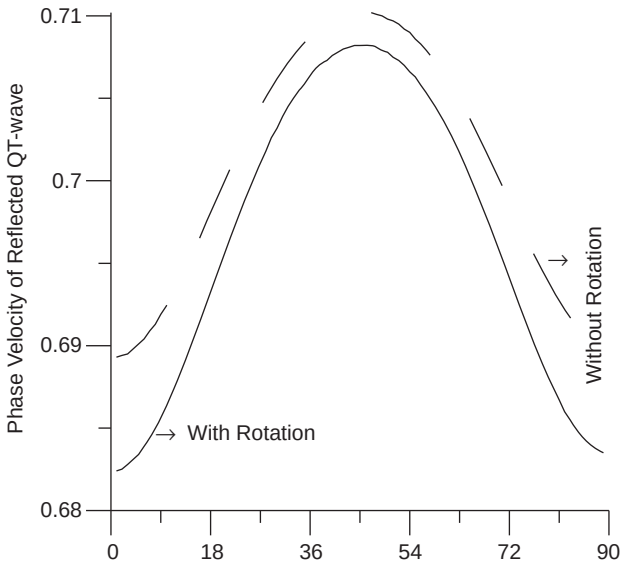

Fig. 4. Angle of incidence (in deg.)

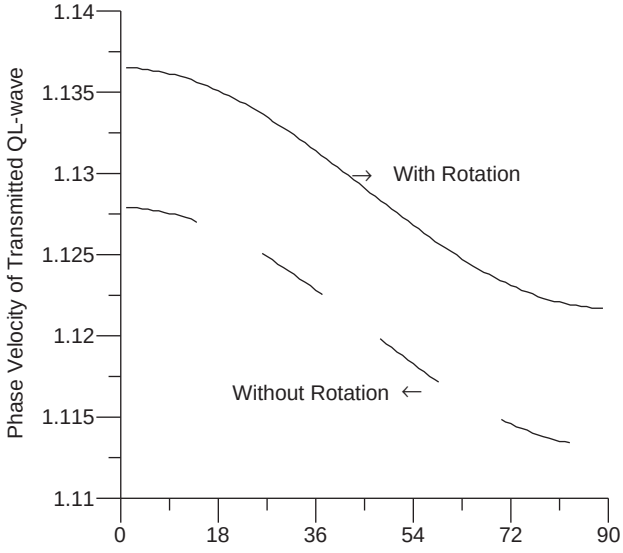

Fig. 5. Angle of incidence (in deg.)

$$b_\ell = 0 \ (\ell = 1,\ldots,6), \quad b_\ell = \left[c'_{44}\left(\frac{\omega \cos e_\ell}{c_\ell}F_\ell - \frac{\omega \sin e_\ell}{c_\ell}\right)\right] \quad (\ell = 7,\ldots,9)$$

$$d_\ell = F^*_\ell \ (\ell = 1,\ldots,6), \quad d_\ell = -F^*_\ell \ (\ell = 7,\ldots,9), \quad f_\ell = 0 \ (\ell = 7,\ldots,9).$$

Welded contact: Welded contact or perfect bonding means continuity of stress components, components of displacement and temperature distribution across the interface and this type of contact has been obtained from boundary conditions given by Eq. (26) by taking $K_n \to \infty$, $K_t \to \infty$, $K_c \to \infty$. The corresponding

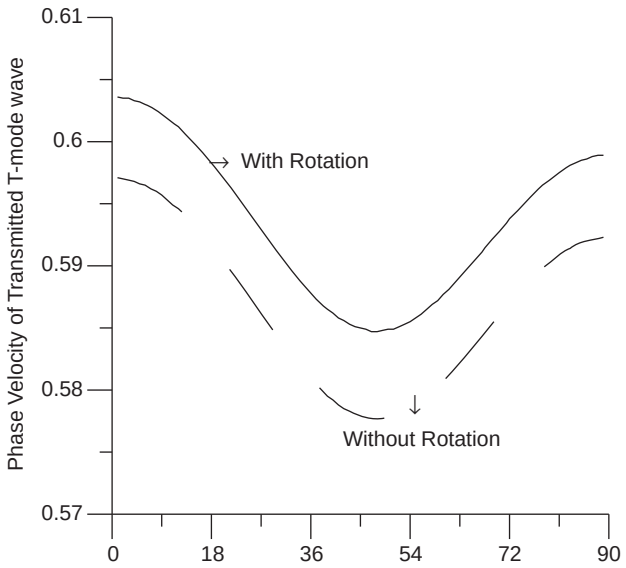

Fig. 6. Angle of incidence (in deg.)

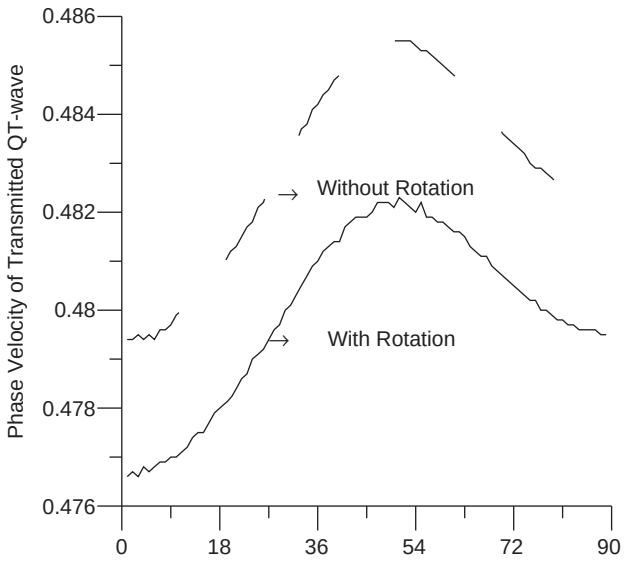

Fig. 7. Angle of incidence (in deg.)

changed values of a_ℓ, b_ℓ and d_ℓ are given by

$$a_\ell = 1 \ (\ell = 1,\ldots,6), \quad a_\ell = -1 \ (\ell = 7,\ldots,9),$$

$$b_\ell = F_\ell \ (\ell = 1,\ldots,6), \quad b_\ell = -F_\ell \ (\ell = 7,\ldots,9),$$

$$d_\ell = F_\ell^* \ (\ell = 1,\ldots,6), \quad d_\ell = -F_\ell^* \ (\ell = 7,\ldots,9).$$

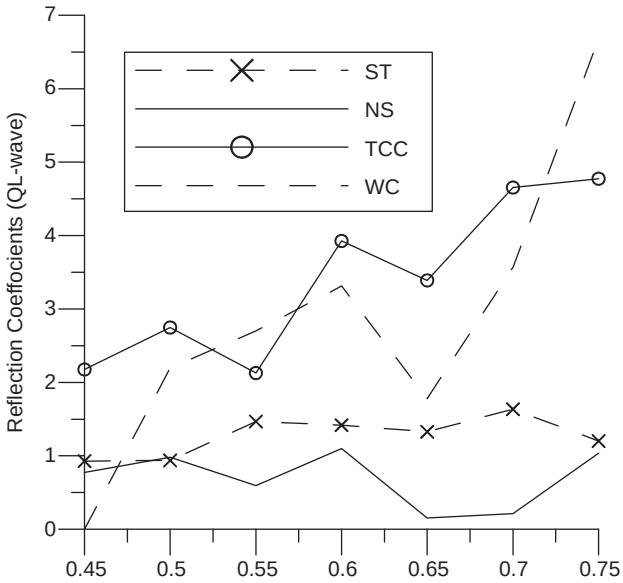

Fig. 8. Variations of amplitude ratios with dimensionless rotation Ω_1 for incident QL-wave: dimensionless rotation.

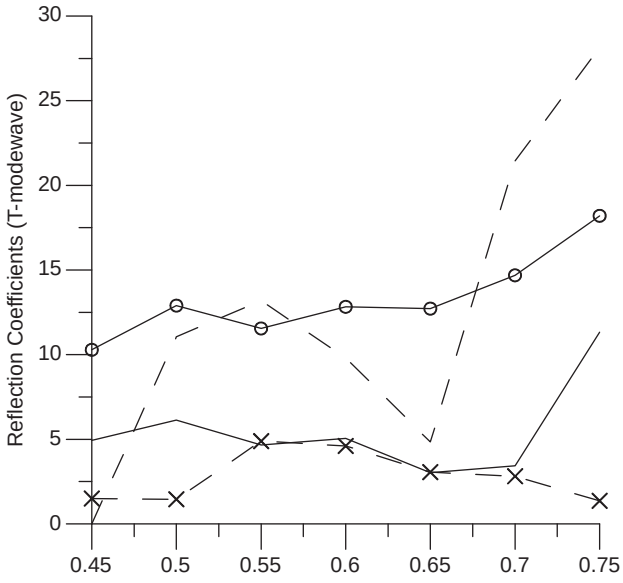

Fig. 9. Variations of amplitude ratios with dimensionless rotation Ω_1 for incident QL-wave: dimensionless rotation.

7. Special cases

1. *Transversely isotropic*: For transversely isotropic generalized thermoelastic rotating medium with axis of symmetry coinciding with x_1-axis, then we have

$$c_{14} = c_{24} = c_{34} = c_{56} = 0, \quad c_{22} = c_{33}, \quad c_{13} = c_{12}, \quad c_{55} = c_{44}, \quad c_{23} = c_{22} - 2c_{44},$$

$$K_2 = K_3,\ \alpha_2 = \alpha_3,\ \beta_1 = c_{11}\alpha_1 + 2c_{12}\alpha_2,\ \beta_2 = \beta_3 = c_{12}\alpha_1 + 2(c_{22} - c_{44})\alpha_2.$$

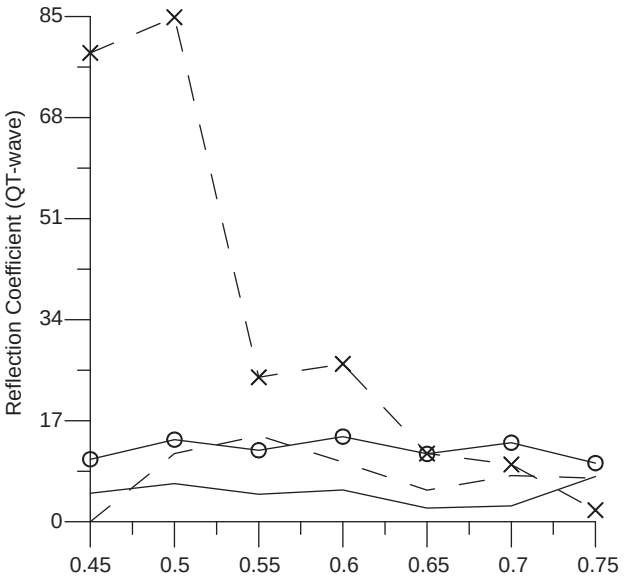

Fig. 10. Variations of amplitude ratios with dimensionless rotation Ω_1 for incident QL-wave: dimensionless rotation.

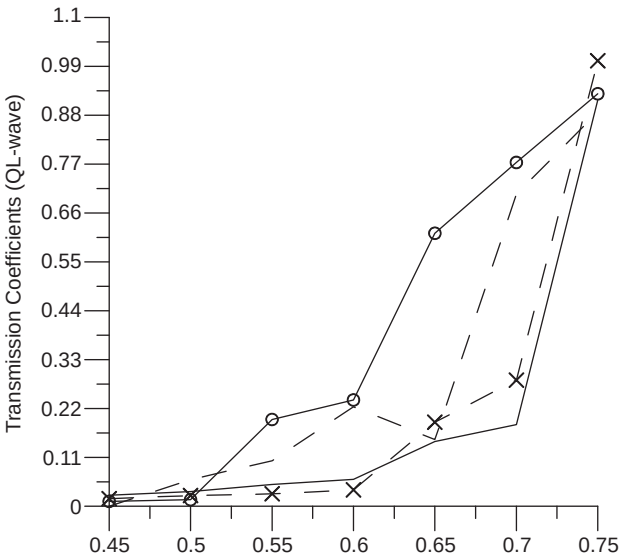

Fig. 11. Variations of amplitude ratios with dimensionless rotation Ω_1 for incident QL-wave: dimensionless rotation.

Using these values, the above results reduced to the case of generalized thermoelastic transversely isotropic materials.

2. *Cubic crystal*: By applying following values for elastic and thermal parameters, our corresponding results reduced to the case of generalized thermoelastic rotating cubic crystal materials.

$$c_{14} = c_{24} = c_{34} = c_{56} = 0, \quad c_{22} = c_{33} = c_{11}, \quad c_{13} = c_{23} = c_{12}, \quad c_{55} = c_{66} = c_{44},$$

$$K_1 = K_2 = K_3 = K^*, \quad \alpha_1 = \alpha_2 = \alpha_3 = \alpha_t, \quad \beta_1 = \beta_2 = \beta_3 = \beta = (c_{11} + 2c_{12})\alpha_t.$$

3. *Isotropic*: For an isotropic generalized thermoelastic rotating medium, we have

$$c_{11} = c_{22} = c_{33} = \lambda + 2\mu, \quad c_{12} = c_{13} = c_{23} = \lambda, \quad c_{44} = c_{55} = c_{66} = \mu,$$

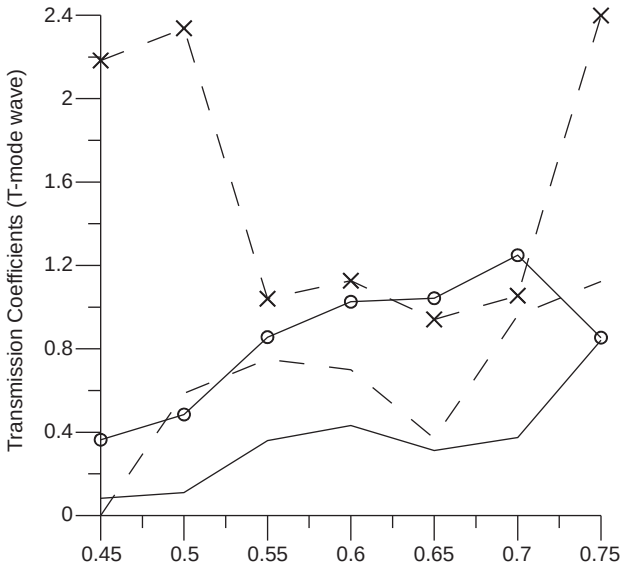

Fig. 12. Variations of amplitude ratios with dimensionless rotation Ω_1 for incident QL-wave: dimensionless rotation.

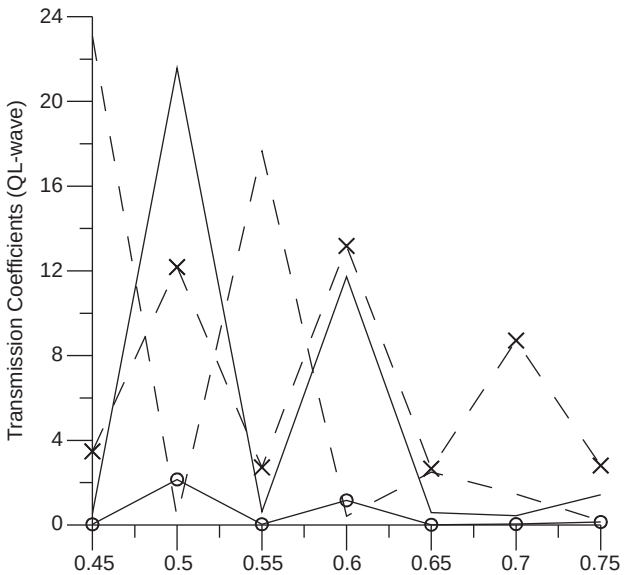

Fig. 13. Variations of amplitude ratios with dimensionless rotation Ω_1 for incident QL-wave: dimensionless rotation.

$$c_{14} = c_{24} = c_{34} = c_{56} = 0, \quad \beta = \beta_1 = \beta_2 = \beta_3 = (3\lambda + 2\mu)\alpha_t$$

$$K_1 = K_2 = K_3 = K^*, \quad \alpha_1 = \alpha_2 = \alpha_3 = \alpha_t.$$

In the foregoing results, if we use the above values of parameters, our problem reduced to the plane wave propagation in generalized thermoelastic isotropic rotating materials. Our results after some modification and simplifications tally with Abd-Alla and Al-Dawy [18] (for free surface in absence or rotation).

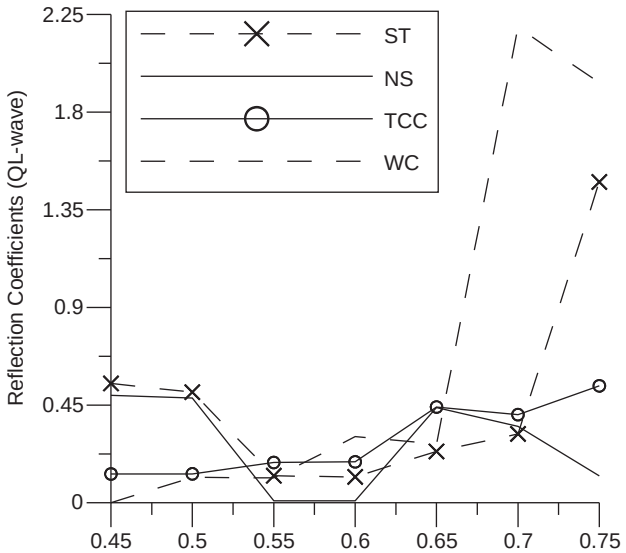

Fig. 14. Variations of amplitude ratios with dimensionless rotation Ω_1 for incident T-mode wave: dimensionless rotation.

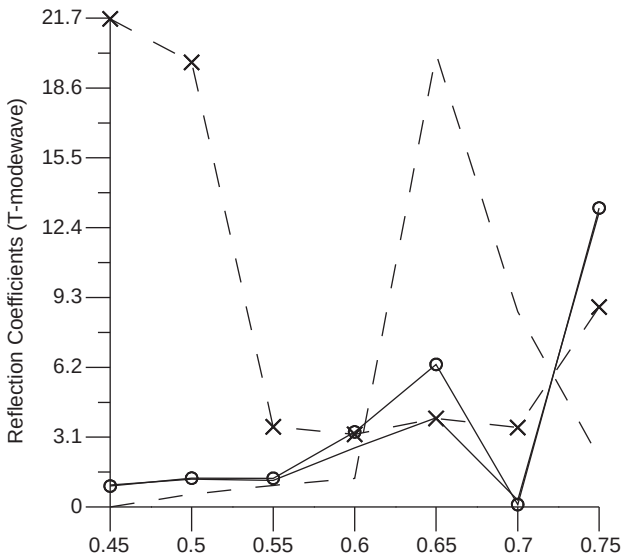

Fig. 15. Variations of amplitude ratios with dimensionless rotation Ω_1 for incident T-mode wave: dimensionless rotation.

8. Numerical results and discussion

In order to illustrate theoretical results in the proceeding sections, we now present some numerical results. The materials chosen for the purpose are Magnesium (M-medium) and Cobalt (M'-medium), the physical data for which are given as [6]

$$
\left.\begin{array}{l}
\text{Magnesium}\\
c_{22}=5.974\times10^{10}\,\mathrm{N\,m^{-2}},\quad c_{44}=3.278\times10^{10}\,\mathrm{N\,m^{-2}},\quad c_{33}=6.17\times10^{10}\,\mathrm{N\,m^{-2}},\\
c_{23}=6.17\times10^{10}\,\mathrm{N\,m^{-2}},\quad \beta_2=2.68\times10^{6}\,\mathrm{N\,m^{-2}\,deg^{-1}},\quad \beta_3=2.68\times10^{6}\,\mathrm{N\,m^{-2}\,deg^{-1}},\\
K_2=1.7\times10^{2}\,\mathrm{W\,m^{-1}\,deg^{-1}},\quad K_3=1.7\times10^{2}\,\mathrm{W\,m^{-1}\,deg^{-1}},\quad \rho=1.74\times10^{3}\,\mathrm{Kg\,m^{-3}},\\
T_0=298\,\mathrm{K},\quad C^*=1.04\times10^{3}\,\mathrm{J\,Kg^{-1}\,deg^{-1}},\quad \tau_0=0.005\\
\text{Cobalt}\\
c'_{22}=3.071\times10^{11}\,\mathrm{N\,m^{-2}},\quad c'_{44}=1.510\times10^{11}\,\mathrm{N\,m^{-2}},\quad c'_{33}=3.581\times10^{11}\,\mathrm{N\,m^{-2}},\\
c'_{23}=1.027\times10^{11}\,\mathrm{N\,m^{-2}},\quad \beta'_2=7.04\times10^{6}\,\mathrm{N\,m^{-2}\,deg^{-1}},\quad \beta'_3=6.90\times10^{6}\,\mathrm{N\,m^{-2}\,deg^{-1}},\\
K'_2=0.690\times10^{2}\,\mathrm{W\,m^{-1}\,deg^{-1}},\quad K'_3=0.690\times10^{2}\,\mathrm{W\,m^{-1}\,deg^{-1}},\quad \rho'=8.836\times10^{3}\,\mathrm{Kg\,m^{-3}},\\
T'_0=298\,\mathrm{K},\ C^{*\prime}=4.27\times10^{2}\,\mathrm{J\,Kg^{-1}\,deg^{-1}},\ \tau'_0=0.001\\
\text{Following non-dimensional parameters have been used for calculation}\\
\dfrac{\omega}{\omega^{*\prime}}=0.01,\quad \dfrac{K_n}{kc_{44}}=20\quad \dfrac{K_t}{kc_{44}}=10,\quad \dfrac{K_c}{kK'_3}=5\quad\text{and}\quad \omega^{*\prime}=\dfrac{C^{*\prime}c'_{22}}{K'_2}.
\end{array}\right\}\quad (*)
$$

Rotation will play its role in the propagation of waves has been shown by comparing the phase velocities of different waves in a rotating and non-rotating orthotropic generalized thermoelastic medium with one relaxation time for different values of incidence angle varying from 0° to 90° at $\Omega_1=0.25$ in Figs. 2–7.

We observe that the phase velocities in case of reflected QL-wave, reflected T-mode wave, transmitted QL-wave and transmitted T-mode wave are greater when propagated through a medium with the concept of rotation, whereas the rotation decrease the phase velocities of reflected QT-wave, Transmitted QT-wave.

So, we conclude that the quasi-transverse wave will propagate slowly in a rotating orthotropic generalized thermoelastic medium with one relaxation time. As we know the transverse waves are considered to be more destructive as compared to longitudinal and thermal waves. So, the concept of rotation in an orthotropic

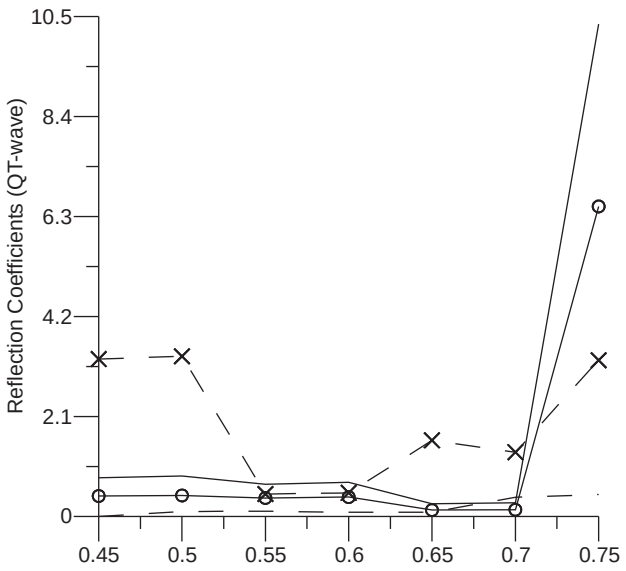

Fig. 16. Variations of amplitude ratios with dimensionless rotation Ω_1 for incident T-mode wave: dimensionless rotation.

thermoelastic medium with one relaxation time, will produce more destruction as compare to non-rotating type.

For the above values of the relevant parameters in (*), the system of Eqs. (34)–(42) is solved for absolute amplitude ratios by using Gauss-elimination method for different values of dimensionless rotation Ω_1 varying from 0.45 to 0.75 at an angle of incidence equal to 45° and then using these absolute amplitude ratios, absolute reflection and transmission coefficients are calculated from Eqs. (43)–(44). i.e. for incident QL-wave, the absolute reflection and transmission coefficients can be written as

$$|R_{PP}| = \left(\frac{1+F_4^2+F_4^{*2}}{1+F_1^2+F_1^{*2}}\right)^{1/2}\left|\frac{B_4}{B_1}\right|, \quad |R_{PT}| = \left(\frac{1+F_5^2+F_5^{*2}}{1+F_1^2+F_1^{*2}}\right)^{1/2}\left|\frac{B_5}{B_1}\right|, \quad |R_{PS}| = \left(\frac{1+F_6^2+F_6^{*2}}{1+F_1^2+F_1^{*2}}\right)^{1/2}\left|\frac{B_6}{B_1}\right|$$

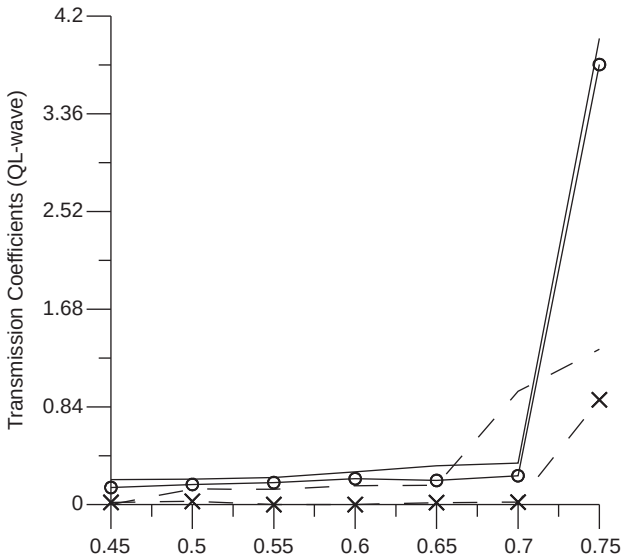

Fig. 17. Variations of amplitude ratios with dimensionless rotation Ω_1 for incident T-mode wave: dimensionless rotation.

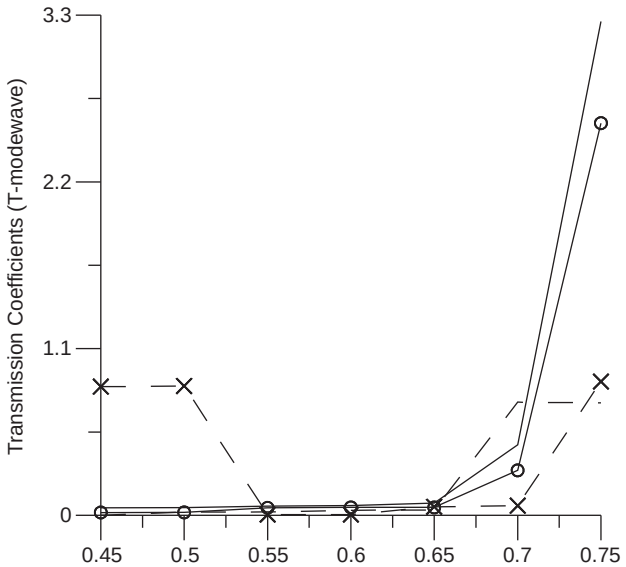

Fig. 18. Variations of amplitude ratios with dimensionless rotation Ω_1 for incident T-mode wave: dimensionless rotation.

and

$$|T_{PP}| = \left(\frac{1+F_7^2+F_7^{*2}}{1+F_1^2+F_1^{*2}}\right)^{1/2}\left|\frac{B_7}{B_1}\right|, \quad |T_{PT}| = \left(\frac{1+F_8^2+F_8^{*2}}{1+F_1^2+F_1^{*2}}\right)^{1/2}\left|\frac{B_8}{B_1}\right|, \quad |T_{PS}| = \left(\frac{1+F_9^2+F_9^{*2}}{1+F_1^2+F_1^{*2}}\right)^{1/2}\left|\frac{B_9}{B_1}\right|.$$

Similar expressions can be written for the reflection and transmission coefficients for incident T-mode and incident QT-waves. A computer program has been developed. The variations of these coefficients for thermoelastic solid with Stiffness (ST), thermoelastic solid with Normal Stiffness (NS), thermoelastic solid with Thermal Contact Conductance (TCC) and thermoelastic solid with Welded Contact (WC) have been shown by dotted line with centre symbol (- × - × - × - × - × -), solid line (————), solid line with centre symbol (-o—o—o-), and dotted line (- - - - - - - - - - - -), respectively, in Figs. 8–25.

The variations of reflection and transmission coefficients have been studied for the three different incident waves as follows.

Incident QL-wave: Fig. 8 shows the variations of reflection coefficient $|R_{PP}|$ with dimensionless rotation Ω_1. The values of $|R_{PP}|$ for TCC, WC are larger than those for ST whereas in case of NS values are smaller than ST. The values of $|R_{PT}|$ are always smaller for ST as compared with TCC, WC, NS and these are shown in Fig. 9.

The variations of reflection coefficient $|R_{PS}|$ are depicted in Fig. 10. The values for ST are greater than those for TCC, WC, NS in the range $0.45 \leqslant \Omega_1 \leqslant 0.65$ and when $0.65 \leqslant \Omega_1 \leqslant 0.75$ the values for ST decrease suddenly. In case of transmission coefficients $|T_{PP}|$ the values for ST are smaller than those for NS, TCC, WC in the range $0.45 \leqslant \Omega_1 \leqslant 0.60$, $0.45 \leqslant \Omega_1 \leqslant 0.70$, $0.45 \leqslant \Omega_1 \leqslant 0.70$, respectively otherwise greater and the variations of these are shown in Fig. 11.

Fig. 12 shows that the values for transmission coefficient $|T_{PT}|$ which are greater than NS, WC for all values of Ω_1, whereas smaller than TCC in the range $0.63 \leqslant \Omega_1 \leqslant 0.70$ only, for ST boundary. The value of transmission coefficient $|T_{PS}|$ in Fig. 13 shows that the values for ST boundary are more than TCC, WC, NS only when Ω_1 lies between $0.57 \leqslant \Omega_1 \leqslant 0.75$ and oscillatory behavior is due to the complex nature of the problem.

Incident T-mode wave: Figs. 14 and 16 depict the variations of reflection coefficients $|R_{TP}|$ and $|R_{TS}|$ with dimensionless rotation Ω_1, respectively. The values for all the reflection coefficients are greater in case of ST as compared with TCC, WC, NS for all values of Ω_1.

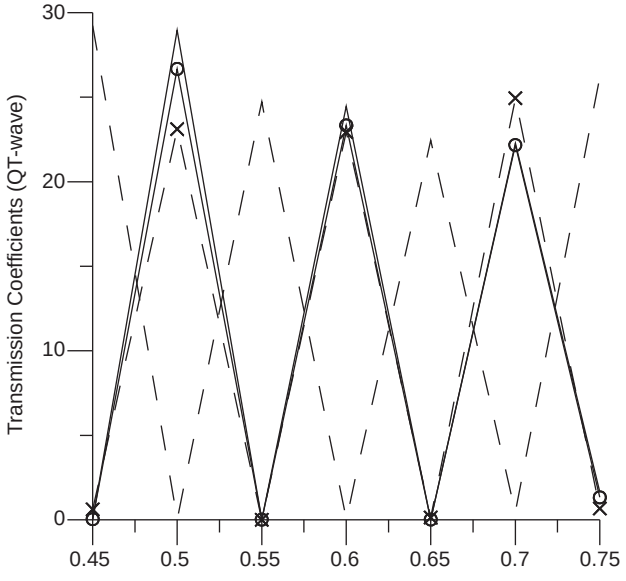

Fig. 19. Variations of amplitude ratios with dimensionless rotation Ω_1 for incident T-mode wave: dimensionless rotation.

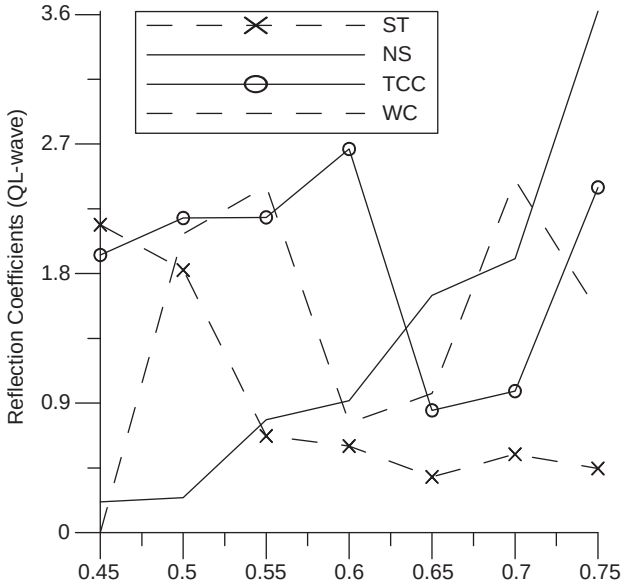

Fig. 20. Variations of amplitude ratios with dimensionless rotation Ω_1 for incident QT-wave: dimensionless rotation.

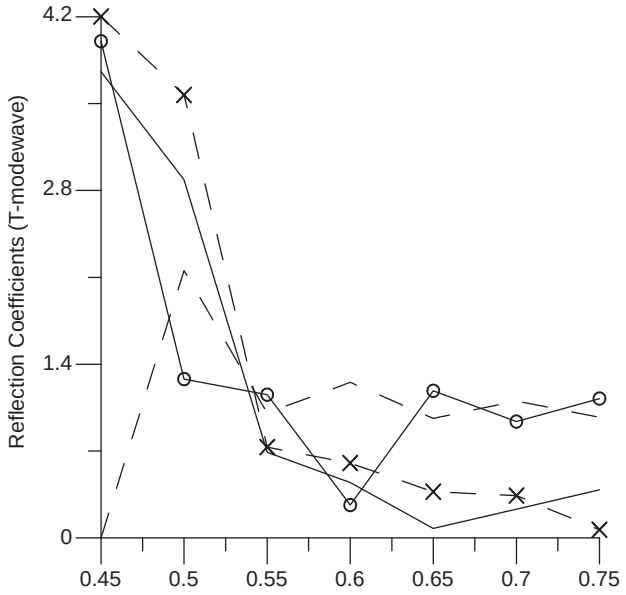

Fig. 21. Variations of amplitude ratios with dimensionless rotation Ω_1 for incident QT-wave: dimensionless rotation.

The values of $|R_{TT}|$, in case of ST boundary are greater than all other boundaries in the range when Ω_1 lies between $0.45 \leqslant \Omega_1 \leqslant 0.60$ and after this range some greater values are observed for other boundaries in different ranges. These are shown in Fig. 15. For incident T-mode wave, the variations of transmission coefficients $|T_{TP}|$ are shown in Fig. 17. It is found that the values of transmission coefficients for ST are always smaller than all other different boundaries. The values for transmission coefficient $|T_{TT}|$ for the case of ST are larger than those for other boundaries in the range $0.45 \leqslant \Omega_1 \leqslant 0.55$ and after that found to be smaller and

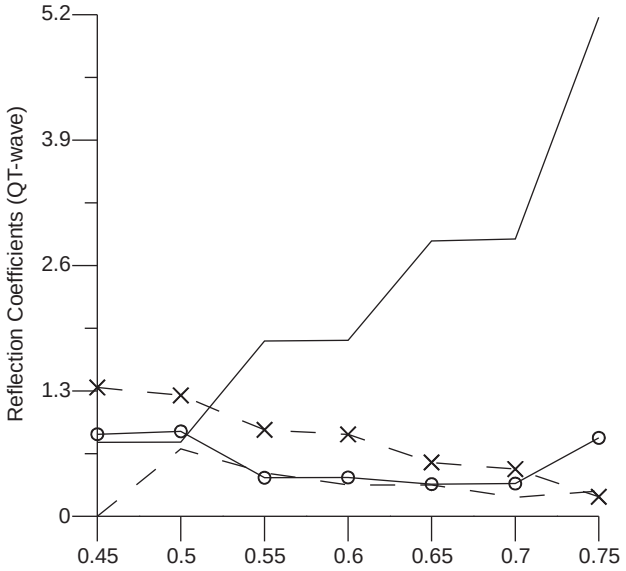

Fig. 22. Variations of amplitude ratios with dimensionless rotation Ω_1 for incident QT-wave: dimensionless rotation.

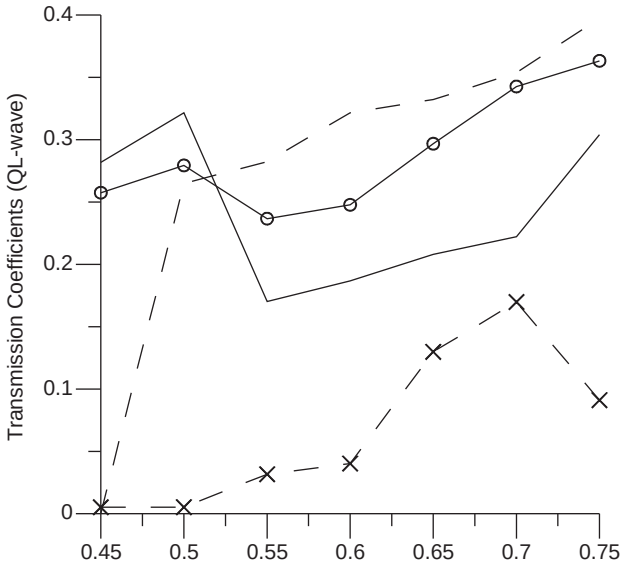

Fig. 23. Variations of amplitude ratios with dimensionless rotation Ω_1 for incident QT-wave: dimensionless rotation.

these are depicted in Fig. 18. Fig. 19 shows the variations of transmission coefficients $|T_{TS}|$. The oscillatory behavior is observed for all the boundaries.

In Figs. 14 and 16 the values for ST are demagnified by dividing the original values by 10, to depict the comparison between the boundaries.

Incident QT-wave: Reflection and transmission coefficients i.e. $|R_{SP}|$, $|R_{ST}|$, $|R_{SS}|$, $|T_{SP}|$, $|T_{ST}|$, $|T_{SS}|$ for dimensionless rotation Ω_1 for incident QT wave are shown in Figs. 20–25, respectively. The values of $|R_{SP}|$ for NS are much greater than those for all other boundaries, whereas the values for ST are smaller than all other

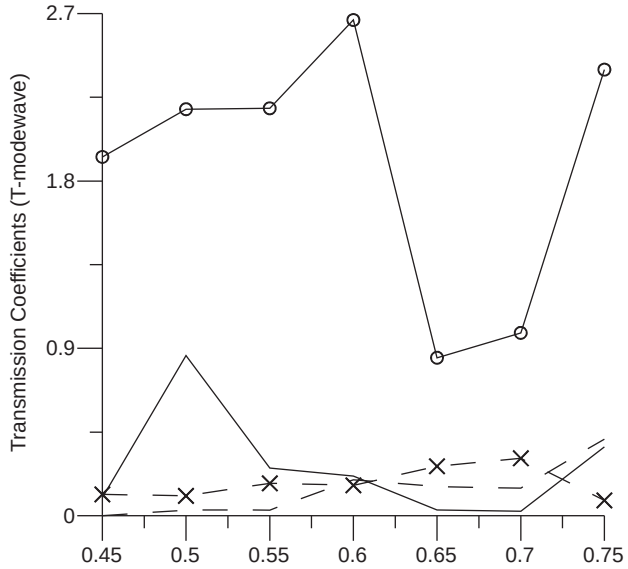

Fig. 24. Variations of amplitude ratios with dimensionless rotation Ω_1 for incident QT-wave: dimensionless rotation.

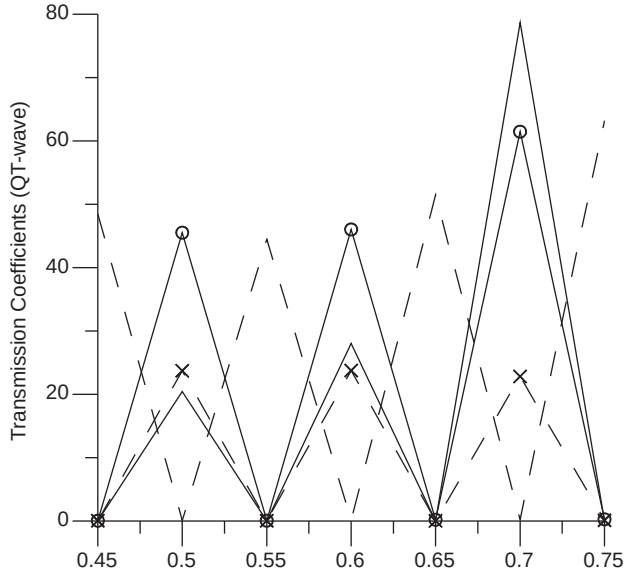

Fig. 25. Variations of amplitude ratios with dimensionless rotation Ω_1 for incident QT-wave: dimensionless rotation.

in the range $0.55 \leqslant \Omega_1 \leqslant 0.75$ only. In case of ST, the values for $|R_{ST}|$ are greater than those for NS; [TCC] and WC when Ω_1 lies between $0.45 \leqslant \Omega_1 \leqslant 0.72$; [$0.45 \leqslant \Omega_1 \leqslant 0.55$, $0.57 \leqslant \Omega_1 \leqslant 0.62$] and $0.45 \leqslant \Omega_1 \leqslant 0.55$, respectively.

The values of reflection coefficient $|R_{SS}|$ for the case of ST are greater than all those for other boundaries except for NS in the range $0.70 \leqslant \Omega_1 \leqslant 0.75$. For the transmission coefficients $|T_{SP}|$, the values in case of ST boundary are smaller than those for NS, TCC, WC for all the values of Ω_1. Fig. 24 shows that the values of transmission coefficient for transmitted T-mode wave i.e. $|T_{ST}|$ in case of TCC are found much higher than all

others whereas the values in case of ST are greater than those for NS and WC in the range $0.62 \leqslant \Omega_1 \leqslant 0.72$ and $0.62 \leqslant \Omega_1 \leqslant 0.71$, respectively.

It is concluded that the trend of variations of transmission coefficients $|T_{SS}|$ is oscillatory and values in case of NS are found to be much higher. To depict the comparison, the values in Figs. 20, 23, 25 for NS are demagnified by dividing the original values by 100, 10, 10 and in Fig. 22 the values for ST are demagnified by dividing the original values by 10.

9. Conclusion

Generalized theory developed by Lord–Shulman [1] is used to study the problem. The analytical expressions of the amplitude ratios for various reflected and transmitted waves are obtained for an Imperfect Boundary and deduced for normal stiffness, transverse stiffness, thermal contact conductance, slip boundary and welded contact. The reflection and transmission coefficients are compared graphically for different incident waves with dimensionless rotation Ω_1. Some particular cases of thermoelastic solids such as transversely isotropic, cubic crystal and isotropic solids has been deduced from the present case of orthotropic thermoelastic rotating solid. It is concluded that rotation effects the propagation of waves in different type of boundaries. Effect of rotation on the phase velocities of waves is also observed in Figs. 2–7 and concluded that the concept of rotation in an orthotropic thermoelastic medium with one relaxation time, will produce more destruction as compare to non-rotating type. It is observed that in case of incident QT-wave the reflection and transmission coefficients for NS boundary are found to be much higher than the others. A theoretical model has been adopted in the present study but it is one of the realistic form of earth model and is useful for further investigation for different seismologists.

Appendix A

$$\Delta = \begin{vmatrix} a_4 & a_5 & a_6 & a_7 & a_8 & a_9 \\ b_4 & b_5 & b_6 & b_7 & b_8 & b_9 \\ d_4 & d_5 & d_6 & d_7 & d_8 & d_9 \\ e_4 & e_5 & e_6 & e_7 & e_8 & e_9 \\ f_4 & f_5 & f_6 & f_7 & f_8 & f_9 \\ g_4 & g_5 & g_6 & g_7 & g_8 & g_9 \end{vmatrix}, \quad \Delta_4^p = \begin{vmatrix} -a_1 & a_5 & a_6 & a_7 & a_8 & a_9 \\ -b_1 & b_5 & b_6 & b_7 & b_8 & b_9 \\ -d_1 & d_5 & d_6 & d_7 & d_8 & d_9 \\ -e_1 & e_5 & e_6 & e_7 & e_8 & e_9 \\ -f_1 & f_5 & f_6 & f_7 & f_8 & f_9 \\ -g_1 & g_5 & g_6 & g_7 & g_8 & g_9 \end{vmatrix},$$

$$\Delta_5^p = \begin{vmatrix} a_4 & -a_1 & a_6 & a_7 & a_8 & a_9 \\ b_4 & -b_1 & b_6 & b_7 & b_8 & b_9 \\ d_4 & -d_1 & d_6 & d_7 & d_8 & d_9 \\ e_4 & -e_1 & e_6 & e_7 & e_8 & e_9 \\ f_4 & -f_1 & f_6 & f_7 & f_8 & f_9 \\ g_4 & -g_1 & g_6 & g_7 & g_8 & g_9 \end{vmatrix}, \quad \Delta_6^p = \begin{vmatrix} a_4 & a_5 & -a_1 & a_7 & a_8 & a_9 \\ b_4 & b_5 & -b_1 & b_7 & b_8 & b_9 \\ d_4 & d_5 & -d_1 & d_7 & d_8 & d_9 \\ e_4 & e_5 & -e_1 & e_7 & e_8 & e_9 \\ f_4 & f_5 & -f_1 & f_7 & f_8 & f_9 \\ g_4 & g_5 & -g_1 & g_7 & g_8 & g_9 \end{vmatrix},$$

$$\Delta_7^p = \begin{vmatrix} a_4 & a_5 & a_6 & -a_1 & a_8 & a_9 \\ b_4 & b_5 & b_6 & -b_1 & b_8 & b_9 \\ d_4 & d_5 & d_6 & -d_1 & d_8 & d_9 \\ e_4 & e_5 & e_6 & -e_1 & e_8 & e_9 \\ f_4 & f_5 & f_6 & -f_1 & f_8 & f_9 \\ g_4 & g_5 & g_6 & -g_1 & g_8 & g_9 \end{vmatrix}, \quad \Delta_8^p = \begin{vmatrix} a_4 & a_5 & a_6 & a_7 & -a_1 & a_9 \\ b_4 & b_5 & b_6 & b_7 & -b_1 & b_9 \\ d_4 & d_5 & d_6 & d_7 & -d_1 & d_9 \\ e_4 & e_5 & e_6 & e_7 & -e_1 & e_9 \\ f_4 & f_5 & f_6 & f_7 & -f_1 & f_9 \\ g_4 & g_5 & g_6 & g_7 & -g_1 & g_9 \end{vmatrix},$$

$$\Delta_9^p = \begin{vmatrix} a_4 & a_5 & a_6 & a_7 & a_8 & -a_1 \\ b_4 & b_5 & b_6 & b_7 & b_8 & -b_1 \\ d_4 & d_5 & d_6 & d_7 & d_8 & -d_1 \\ e_4 & e_5 & e_6 & e_7 & e_8 & -e_1 \\ f_4 & f_5 & f_6 & f_7 & f_8 & -f_1 \\ g_4 & g_5 & g_6 & g_7 & g_8 & -g_1 \end{vmatrix},$$

Δ_4^T and Δ_4^S are obtained from Δ_4^p on replacing the elements $(-a_1, -b_1, -d_1, -e_1, -f_1, -g_1)$ by $(-a_2, -b_2, -d_2, -e_2, -f_2, -g_2)$ and $(-a_3, -b_3, -d_3, -e_3, -f_3, -g_3)$. Δ_ℓ^T and Δ_ℓ^S $(\ell = 5, 6, 7, 8, 9)$ are defined similarly.

References

[1] H.W. Lord, Y. Shulman, A generalized dynamical theory of thermoelasticity, *J. Mech. Phys. Solids* 15 (1967) 299–309.
[2] J.P. Jones, J.P. Whittier, Waves in a flexible bonded interface, *J. Appl. Mech.* 34 (1967) 905–909.
[3] A.E. Green, K.A. Lindsay, Thermoelasticity, *J. Elasticity* 2 (1) (1972) 1–7.
[4] A.H. Nayfeh, E.M. Nassar, Simulation of the influence of bonding materials on the dynamic behaviour of laminated composites, *J. Appl. Mech.* 45 (1978) 828–855.
[5] S.I. Rokhlin, M. Hefets, M. Rosen, An elastic interface wave guided by a thin film between two solids, *J. Appl. Phys.* 51 (1980) 3579–3582.
[6] R.S. Dhaliwal, A. Singh, *Dynamical Coupled Thermoelasticity*, Hindustan Publishers, Delhi, 1980.
[7] R.S. Dhaliwal, H.H. Sherief, Generalized thermoelasticity for anisotropic media, *Q. Appl. Math.* 38 (1980) 1–8.
[8] S.I. Rokhlin, Adhesive joint characterization by ultrasonic surface and interface waves, in: K.L. Mittal (Ed.), *Adhesive Joints: Formation, Characteristics and Testing*, Plenum, New York, 1984, pp. 307–345.
[9] J.M. Baik, R.B. Thompson, Ultrasonic scattering from imperfect interfaces a quasi-static model, *J. Nondestr. Eval.* 4 (1984) 177–196.
[10] T.C. Angel, J.D. Achenbach, Reflection and transmission of elastic waves by a periodic array of crack, *J. App. Mech.* 52 (1985) 33–41.
[11] S.I. Rokhlin, D. Marom, Study of adhesive bonds using low-frequency obliquely incident ultrasonic wave, *J. Acoust. Soc. Am.* 80 (1986) 585–590.
[12] A. Pilarski, J.L. Rose, A transverse wave ultrasonic oblique-incidence technique for interface weakness detection in adhesive bonds, *J. Appl. Phys.* 63 (1988) 300–307.
[13] J.N. Sharma, Reflection of thermoelastic waves from the stress-free insulated boundary of an anisotropic half-space, *Indian J. Pure Appl. Math.* 19 (3) (1988) 294–304.
[14] J.N. Sharma, H. Singh, Generalized thermoelastic waves in anisotropic media, *J. Acoust. Soc. Am.* 85 (4) (1989) 1407–1412.
[15] S.B. Sinha, K.A. Elasibai, Reflection of thermoelastic waves at a solid half-space with two relaxation times, *J. Therm. Stresses* 19 (1996) 749–762.
[16] S.B. Sinha, K.A. Elasibai, Reflection and refraction of thermoelastic waves at an interface of two semi-infinite media with two relaxation times, *J. Therm. Stresses* 20 (1997) 129–145.
[17] A.I. Lavrentyev, S.I. Rokhlin, Ultrasonic spectroscopy of imperfect contact interfaces between a layer and two solids, *J. Acoust. Soc. Am.* 103 (2) (1998) 657–664.
[18] A.N. Abd-Alla, A.A.S. Al-Dawy, The reflection phenomena of SV-waves in generalized thermoelastic medium, *Int. J. Math Math Sci.* 23 (8) (2000) 529–546.
[19] K.L. Verma, On the propagation of waves in layered anisotropic media in generalized thermoelasticity, *Int. J. Eng. Sci.* 40 (2002) 2077–2096.
[20] B. Singh, Wave propagation in an anisotropic generalized thermoelastic solid, *Indian J. Pure Appl. Math.* 34 (10) (2003) 1479–1485.
[21] M.I.A. Othman, Effect of rotation on plane waves in generalized thermo-elasticity with two relaxation times, *Int. J. Solids Struct.* 41 (11–12) (2004) 2939–2956.
[22] S. Leungvichcharoen, A.C. Wijeyewickrema, T. Yamamato, Axi-symmetric waves in pre-stressed imperfectly bonded incompressible elastic layered composites, *Int. J. Solids Struct.* 41 (24–25) (2004) 6873–6894.
[23] R. Kumar, J.N. Sharma, Reflection of plane waves from the boundaries of a micropolar thermoelastic half-space without energy dissipation, *Int. J. Appl. Mech. Eng.* 10 (4) (2005) 631–645.
[24] X. Wang, J. Zhang, X. Guo, Two circular inclusions with inhomogeneously imperfect interfaces in plane elasticity, *Int. J. Solids Struct.* 42 (2005) 2601–2623.
[25] M.I.A. Othman, Effect of rotation and relaxation times on a thermal shock for a half-space in generalized thermo-viscoelasticity, *Acta Mech.* 174 (3–4) (2005) 129–143.
[26] A. Baksi, R.K. Bera, Relaxation effects on plane wave propagation in a rotating magneto-thermo-viscoelastic medium, *J. Therm. Stresses* 29 (2006) 753–769.

[27] J.N. Sharma, M.D. Thakur, Effect of rotation on Rayleigh–Lamb waves in magneto-thermoelastic media, *J. Sound Vib.* 296 (4–5) (2006) 871–887.
[28] S. Ueda, S. Biwa, K. Watanabe, R. Heuer, C. Pecorari, On the stiffness of spring model for closed crack, *Int. J. Eng. Sci.* 44 (2006) 874–888.
[29] J.N. Sharma, M.I.A. Othman, Effect of rotation on generalized thermo-viscoelastic Rayleigh–Lamb waves, *Int. J. Solids Struct.* 44 (13–15) (2007) 4243–4255.